The International Journal of Cardiovascular Imaging (2019) 35:665–673
https://doi.org/10.1007/s10554-018-1492-0

ORIGINAL PAPER

Increased fractal dimension of left ventricular trabeculations is associated with subclinical diastolic dysfunction in patients with type-2 diabetes mellitus

Yongning Shang[1] · Xiaochun Zhang[1] · Weiling Leng[2] · Xiaotian Lei[2] · Liu Chen[2] · Xiaoyue Zhou[3] · Kelvin Chow[4] · Yanshu Shi[1] · Jianlong Dong[1] · Ziwen Liang[2] · Jian Wang[1]

Received: 9 July 2018 / Accepted: 31 October 2018 / Published online: 14 November 2018

Abstract

The aim of this study was to investigate the relationship among left ventricular (LV) concentric hypertrophy, endocardial remodeling, and myocardial deformation in type-2 diabetes mellitus (T2DM). Fifty-three T2DM patients with normotension and 36 healthy controls underwent cardiovascular magnetic resonance imaging to assess for LV concentric hypertrophy (LV myocardial mass index, LVMMi; LVMMi-to-LV end-diastolic volume index ratio, MVR), endocardial remodeling (fractal dimension of trabeculations, FD), and myocardial deformation (global longitudinal, radial and circumferential strain, systolic and diastolic strain rate). When compared with healthy controls, T2DM was associated with LV concentric hypertrophy (LVMMi: T2DM, 52.7 ± 8.9 g/m^2; controls, 48.7 ± 8.4 g/m^2, p = 0.032; MVR: T2DM, 0.88 ± 0.19 g/mL; controls, 0.77 ± 0.16 g/mL, p = 0.007), endocardial remodeling (max. apical FD: T2DM, 1.265 ± 0.056; controls, 1.233 ± 0.055, p = 0.008; mean apical FD: T2DM, 1.198 ± 0.043; controls, 1.176 ± 0.043, p = 0.020), and subtle diastolic dysfunction (peak longitudinal diastolic strain rate, PDSRL: T2DM, 1.1 ± 0.2/s; controls, 1.2 ± 0.3/s, p = 0.031). In the stepwise multivariable regression model, the MVR was an independent determinant of the maximum apical FD (standardized β, sβ = 0.525, p < 0.001) and mean apical FD (sβ = 0.568, p < 0.001). The mean apical FD was an independent determinant of the PDSRL (p = 0.004). LV concentric hypertrophy is an independent determinant of endocardial remodeling, a process that may contribute to subtle LV diastolic dysfunction in T2DM patients.

Keywords Type-2 diabetes mellitus · Endocardial remodeling · Fractal dimension of trabeculations · Concentric hypertrophy · Myocardial deformation

✉ Xiaochun Zhang
zxcylxyr@163.com

✉ Ziwen Liang
ziwenliang99@163.com

✉ Jian Wang
wangjian_811@yahoo.com

[1] Department of Radiology, Southwest Hospital, Third Military Medical University (Army Medical University), Gaotanyan Street No. 30, Shapingba District, Chongqing, China

[2] Department of Endocrinology, Southwest Hospital, Third Military Medical University (Army Medical University), Gaotanyan Street No. 30, Shapingba District, Chongqing, China

[3] MR Collaboration, Siemens Healthcare Ltd., Shanghai, China

[4] Cardiovascular MR R&D, Siemens Medical Solutions USA, Inc., Chicago, USA

Introduction

Type-2 diabetes mellitus (T2DM) patients are at increased risk for heart failure [1], and particularly for left ventricular (LV) heart failure with preserved ejection fraction (HFPEF) [2], even in the absence of hypertension and coronary artery disease [3]. The reasons for this remain unclear, but one possible mechanism is cardiac structural remodeling [4]. LV concentric hypertrophy, which is frequently diagnosed in T2DM patients, has been determined to be a strong predictor of HFPEF and other adverse cardiovascular events [5].

LV concentric hypertrophy is characterized by an increased LV mass index and mass-to-end-diastolic volume ratio (MVR) [4, 6]. Mechanically, hypertrophied myocardium can increase the stiffness of the LV wall, and when the decreased passive elasticity of the LV wall becomes incapable of meeting the work load, clinical

HFPEF ensues. Whether there is another precise mechanism underlying LV concentric hypertrophy-mediated LV diastolic dysfunction remains unclear, as mentioned previously, and the underlying mechanism could be endocardial remodeling. Previously, endocardial remodeling could be characterized by the papillary muscle and trabeculations (PMT) mass index (PMTMi) and PMTMi-LV mass index (LVMMi) ratio (PMTMi/LVMMi). Recently, fractal dimension (FD), a unitless number derived from fractal analysis on cardiovascular magnetic resonance (CMR) LV cine images and focused on PMT, has been employed to quantify the complexity of the endocardium [7]. Previous studies indicated that LV hypertrophy is associated with increased endocardial complexity [8], which subsequently contributes to subclinical myocardial dysfunction [9] in healthy populations. However, whether T2DM is associated with increased endocardial complexity or if endocardial remodeling can mediate the effects of LV hypertrophy on LV dysfunction, remains unclear and is a topic worthy of investigation. LV subclinical diastolic and systolic dysfunction can be detected by myocardial mechanics. Recently, CMR tissue tracking technique has been increasingly used for myocardial mechanics measurements in different types of cardiovascular disease due to its higher signal-to-noise ratio than speckle tracking echocardiography and faster post-processing on routine cine images without requiring any additional scan time [10, 11]. Prior studies have yielded conflicting results regarding the effect of T2DM on LV myocardial mechanics [12, 13].

Therefore, we used CMR techniques, including cine, tissue tracking and fractal analysis, to assess the relationship between LV concentric hypertrophy, interstitial fibrosis, endocardial remodeling, and subclinical dysfunction in T2DM.

Methods

Study patients

Fifty-three patients were prospectively enrolled between June 2015 and March 2018. The inclusion criteria were as follows: (1) an initial diagnosis of T2DM, according to World Health Organization criteria [14]; (2) no history of cardiovascular disease or chest pain, and (3) a region of interest (ROI) on T1 maps in which the larger of the two PMs is greater than 0.2 cm^2 [15]. The exclusion criteria included: (1) hypertension (resting systolic blood pressure > 140 mmHg or diastolic blood pressure > 90 mmHg), (2) glomerular filtration rate (GFR) ≤ 30 mL/min/1.7 m^2, and (3) other standard contraindications to cardiac MR. Forty controls were recruited for the study.

Anthropometry and biochemistry exams

All the patients and controls underwent height, weight, and blood pressure measurements. Blood samples were collected about 30 min before the CMR scanning was performed and were immediately sent to the Department of Nuclear Medicine and Clinical Laboratory for analysis of the blood urea nitrogen, creatinine, cystatin C, total cholesterol, triglycerides, high-density lipoprotein cholesterol, low-density lipoprotein cholesterol, glucose, glycated hemoglobin (HbA1c), and hematocrit (HCT).

Cardiac magnetic resonance protocols

All CMR was performed on a 3T MAGNETOM Trio MR scanner (Siemens Healthcare, Erlangen, Germany) with a 6-channel body array coil plus 6 channels from the spine array coil. A prototype target shimming method for patient-specific, localized shimming in the heart was used to improve field uniformity.

Short-axis cine imaging covering the entire LV and four-chamber long-axis cine imaging were performed using an electrocardiogram (ECG)-gated, breath-hold balanced, steady-state free-precession (bSSFP) sequence with the following parameters: slice thickness = 6 mm, gap = 1.5 mm, field of view (FOV) = 325 × 400 mm^2, matrix = 179 × 256, TR/TE = 59.22/1.45 ms, and 25 reconstructed phases per cardiac cycle.

Segmented late gadolinium enhancement (LGE) images were obtained using the phase-sensitive inversion recovery (PSIR) sequence (TR/TE = 680/1.94 ms, slice thickness = 8 mm, and FOV = 325 × 400 mm^2), approximately 10 min after a bolus administration of 0.2 mmol/kg gadoteric acid meglumine (Dotarem, Guerbet, BP7400, F95943, Roissy CdG Cedex, France).

A breath-hold ECG-gated, MOdified Look-Locker Inversion recovery (MOLLI) prototype sequence with a 5b(3b)3b and 4b(1b)3b(1b)2b sampling pattern was performed for native and post-contrast T1 mapping, respectively, with a bSSFP readout, FOV = 400 × 300 mm^2, matrix = 256 × 166, TR/TE = 301.7/1.09 ms, flip angle = 35 degrees, and 6 mm thickness. Mid-ventricular short-axis images were acquired before and approximately 15 min after the administration of contrast. T1 maps were generated inline from the MOLLI images with motion correction (MOCO).

All the cine and T1 maps were transferred to the cvi42 software (Circle Cardiovascular Imaging Inc., Calgary, Alberta, Canada) for offline analysis. Endo- and epicardial contours on the cine images were manually traced to obtain the LV end-diastolic volume index (EDVi),

Table 1 Anthropometry and biochemical characteristics of all participants

	Control (n = 36)	T2DM (n = 53)	p Value
Anthropometry			
Age (year)	51.2 ± 12.1	54.3 ± 7.9	0.152
Diabetic duration (year)		7 [4–11]	
Male [n (%)]	17 (47)	28 (53)	0.270
Height (m)	1.6 ± 0.1	1.6 ± 0.1	0.961
Weight (kg)	62.9 ± 10.2	64.9 ± 10.5	0.379
Body mass index (kg/m^2)	23.8 ± 2.9	24.5 ± 2.9	0.220
Body surface area (m^2)	1.7 ± 0.2	1.7 ± 0.2	0.476
Systolic blood pressure (mmHg)	116.9 ± 9.4	120.1 ± 10.1	0.133
Diastolic blood pressure (mmHg)	80.4 ± 6.9	80 ± 7.3	0.792
Biochemical exam			
Blood urea nitrogen (mmol/L)	5.9 ± 1.5	6.3 ± 2.8	0.458
Creatinine (μmol/L)	63.4 ± 16.5	68 ± 19.2	0.300
Cystatin C (mg/L)	0.8 ± 0.2	0.8 ± 0.2	0.202
Total cholesterol (mmol/L)	5.5 ± 1.8	5.0 ± 1.6	0.237
Triglycerides (mmol/L)	1.5 [0.9, 2.0]	2.1 [1.0, 3.2]	0.046
HDL (mmol/L)	1.5 ± 0.4	1.2 ± 0.4	0.002
LDL (mmol/L)	3.6 ± 1.4	3.0 ± 1.0	0.054
Glucose (mmol/L)	5.3 [5.0, 5.9]	8.4 [6.5, 10.6]	< 0.001
Glycated hemoglobin (%)	5.6 [5.2, 5.8]	7.9 [6.7, 9.3]	< 0.001
Hematocrit (%)	41.8 ± 4.3	39.5 ± 4.4	0.016
Medications			
Angiotensin-converting enzyme inhibitors [n (%)]		7 (13)	
Statins [n (%)]		27 (51)	
Aspirin [n (%)]		8 (15)	

HDL high-density lipoprotein cholesterol, *LDL* low-density lipoprotein cholesterol

end-systolic volume index (ESVi), stroke volume index (SVi), ejection fraction (EF), cardiac index (CI), MMi with PM included in the LV lumen, and PMTMi [16].

Two-dimensional feature tracking was performed on four-chamber long-axis cine images and mid-ventricular short-axis cine images. Endo- and epicardial contours of end diastole were manually delineated before being automatically propagated to all the other phases. The contours were checked, and when poorly tracked, the data of the participant in question was excluded. The LV global longitudinal, circumferential, and radial strain, and the peak systolic and diastolic strain rates were subsequently obtained.

For T1 analysis, an ROI was selected manually on the middle third of the myocardial interventricular septum to avoid epicardial and endocardial partial-volume effects. Another ROI was manually drawn with care in the LV cavity to avoid the papillary muscles and myocardium. A third ROI was manually drawn in the larger of the two PM in the mid-ventricular short-axis slice with care to avoid offset from the blood-myocardial boundary. To minimize potential-partial volume effects from the blood pool, only ROIs on PM greater than 0.2 cm^2 was analyzed. Native and post-contrast T1 values of the LV blood pool, myocardium, and PM were obtained. The extracellular volume (ECV) of the myocardium and PM were calculated from native and post-contrast T1 maps using the published formula [17].

The FD was calculated for each slice in the LV short-axis stack using cvi42 post processing software (prototype 5.3.8) and previously described methodologies [18]. The most apical ventricular section was excluded from all the analyses because of partial-volume effects. The maximal basal and apical FD were separately derived from the basal and apical half of the LV stack.

Inter- and intra-observer reproducibility

To assess inter-observer reproducibility, images of ten randomly selected controls (five men and five women) and ten patients (five men and five women) were independently analyzed by two radiologists (Shang Y and Zhang X, each with more than 3 years' experience). For intra-observer reproducibility, one radiologist (Shang Y) reanalyzed images of the same twenty participants after 1 month.

Table 2 LV geometry, function, T1 values, ECV, and FD of all the participants

	Control (n = 36)	T2DM (n = 53)	p Value
LVEDVi (mL/m^2)	64.3 ± 9.8	61.3 ± 8.7	0.136
LVESVi (mL/m^2)	26.9 ± 6.2	25.6 ± 5.7	0.304
LVSVi (mL/m^2)	37.4 ± 5.5	35.7 ± 5.1	0.150
LVEF (%)	58.4 ± 5.2	58.5 ± 5.3	0.919
CI (L/min/m^2)	2.8 ± 0.5	2.7 ± 0.4	0.548
Heart rate (b/min)	74.4 ± 9.0	76.9 ± 10.0	0.245
LVMMi (g/m^2)	48.7 ± 8.4	52.7 ± 8.9	0.032
MVR (g/mL)	0.77 ± 0.16	0.88 ± 0.19	0.007
PMTMi (g/m^2)	3.5 ± 1.1	4.0 ± 1.6	0.145
PMTMi/MMi (%)	6.7 ± 1.4	6.9 ± 2.1	0.519
LV native T1 (ms)	1225.9 ± 48.3	1237.2 ± 72.5	0.413
LV p-con T1 (ms)	539.2 ± 45.5	526.4 ± 65.4	0.312
LVECV (%)	26.7 ± 2.7	28.7 ± 3.3	0.005
PM native T1 (ms)	1166.7 ± 58.8	1185.8 ± 77.2	0.214
PM p-con T1 (ms)	512.9 ± 37.2	509.4 ± 60.4	0.753
PMECV (%)	28.1 ± 3.4	29.4 ± 3.6	0.082
Global FD	1.200 ± 0.032	1.213 ± 0.034	0.094
Max. basal FD	1.320 ± 0.046	1.335 ± 0.050	0.144
Mean basal FD	1.215 ± 0.044	1.217 ± 0.040	0.815
Max. apical FD	1.233 ± 0.055	1.265 ± 0.056	0.008
Mean apical FD	1.176 ± 0.043	1.198 ± 0.043	0.020

LVEDVi left ventricular end-diastolic volume index, *LVESVi* left ventricular end-systolic volume index, *LVSVi* left ventricular stroke volume index, *CI* cardiac index, *LVMMi* left ventricular myocardial mass index, *MVR* LV mass/EDV, *PMTMi* papillary muscles and trabeculations mass index, *LV p-con T1* left ventricular post-contrast T1, *LVECV* left ventricular extracellular volume, *PMECV* papillary muscle extracellular volume, *FD* fractal dimension

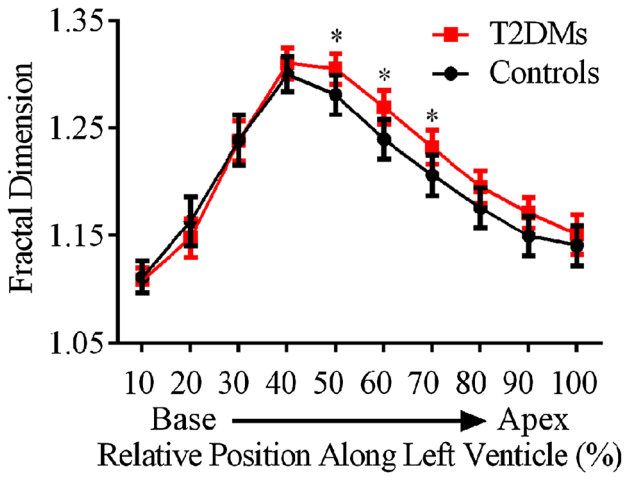

Fig. 1 Graph shows a comparison of the FD between the controls and T2DMs. Heavy central lines represent means of the FD by linear interpolation, and error bars represent 95% confidence interval of the mean for each population

Statistical analysis

Categorical data were presented as percentages. The Kolmogorov–Smirnov test was used to test the normality of the variables. Data that did not fit normality were summarized as medians (interquartile range). Continuous and normal variables were presented as means with standard deviations (SD). Differences between the means were compared using the two tailed unpaired *t* test. The relationship between bivariates was analyzed using linear regression. Variables that were statistically significant in the univariable analyses were entered in the multivariable stepwise linear regression to analyze the independent relationship between FD and LV mechanics. The intra- and inter-observer variabilities for the ECV, thickness, and strain were analyzed by determining the intra-class correlation coefficient (ICC). Statistical tests were two-tailed, and the statistical significance was defined as $p < 0.05$. The data were analyzed using SPSS (version 21.0, SPSS Inc., Chicago, IL, USA) and GraphPad Prism (version 6.01, GraphPad Software, Inc., La Jolla, CA, USA).

Results

Participant characteristics

The demographic, biochemical, and clinical data are summarized in Table 1. T2DM patients (28 male; mean age, 54.3 ± 7.9 years; median diabetes duration, 7 years [interquartile range 4–11]) had similar age, gender, height, weight, body mass index, and blood pressure to the controls subjects (17 male; mean age, 51.2 ± 12.1 years). The T2DM patients were associated with higher triglycerides, glucose and HbA1c, lower HDL, and HCT, and similar blood urea nitrogen, creatinine, cystatin C, total cholesterol, and LDL measurements compared to controls.

Effect of T2DM on left ventricular trabeculations and papillary muscles

T2DM patients had a larger max. apical FD (T2DM, 1.265 ± 0.056; controls, 1.233 ± 0.055, p = 0.008, Table 2) and mean apical FD (T2DM, 1.198 ± 0.043; controls, 1.176 ± 0.043, p = 0.020, Table 2). The global FD, max. basal FD, and mean basal FD were similar between the two groups (Table 2).

The distribution of the FD regarding relative position along the LV is presented in Fig. 1. The greatest differences in the FD between the T2DM patients and controls were registered in the middle LV, located in normalized slices 5–7. In the basal LV (normalized slices 1–4) and apical LV

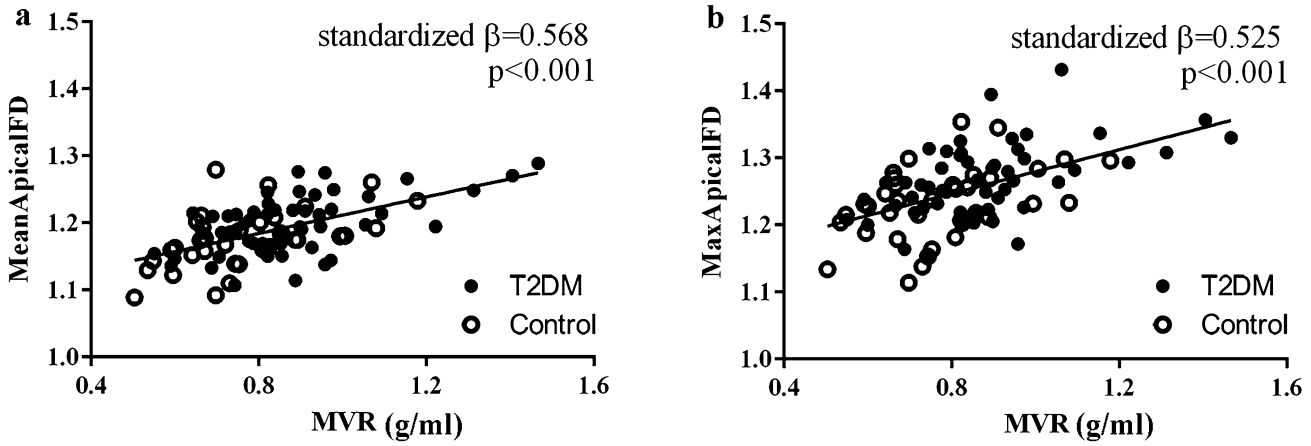

Fig. 2 Relationship between LV concentric hypertrophy and endocardial remodeling. Increased MVR is associated with an elevated mean apical fractal dimension (FD, **a**) and max. apical FD (**b**)

Table 3 LV mechanics measured by feature tracking of all the participants

	Control (n = 36)	T2DM (n = 53)	p Value
PSR (%)	39.9 ± 9.5	38.1 ± 9.3	0.370
PSC (%)	− 21.0 ± 2.7	− 20.1 ± 3.0	0.157
PSSRR (1/s)	2.4 ± 0.8	2.4 ± 0.9	0.764
PSSRC (1/s)	− 1.2 ± 0.2	− 1.2 ± 0.3	0.804
PDSRR (1/s)	− 2.8 ± 1.0	− 2.7 ± 0.9	0.580
PDSRC (1/s)	1.4 ± 0.4	1.3 ± 0.4	0.290
PSL (%)	− 19.8 ± 3.5	− 19.0 ± 3.5	0.305
PSSRL (1/s)	− 1.2 ± 0.2	− 1.2 ± 0.3	0.914
PDSRL (1/s)	1.2 ± 0.3	1.1 ± 0.2	0.031

PSR peak strain radial, *PSC* peak strain circumf., *PSSRR* peak systolic strain rate radial, *PSSRC* peak systolic strain rate circumf., *PDSRR* peak diastolic strain rate radial, *PDSRC* peak diastolic strain rate circumf., *PSL* peak strain long., PSSRL peak systolic strain rate long., *PDSRL* peak diastolic strain rate long., *circumf.* circumferential, *long*. longitudinal

(normalized slices 8–10), there were no differences in the FD between the T2DM patients and controls.

The max. apical FD was associated with the MMi (standardized β, sβ = 0.254, p = 0.016), EDVi (sβ = − 0.426, p < 0.001), and MVR (sβ = 0.525, p < 0.001), but not with age, BMI, PMECV, or LVECV (all p > 0.05). The mean apical FD was also associated with the MMi (sβ = 0.348, p = 0.001), EDVi (sβ = − 0.372, p < 0.001), and MVR (sβ = 0.568, p < 0.001). In the stepwise multivariable linear regression model, MVR was an independent determinant of the max. apical FD (sβ = 0.525, p < 0.001, Fig. 2a) and mean apical FD (sβ = 0.568, p < 0.001, Fig. 2b).

T2DM patients demonstrated similar PM native T1, post-contrast T1, ECV, PMTMi, and PMTMi/MMi to the controls (Table 2).

Effect of T2DM on left ventricular myocardium

The LVMMi was greater in the T2DM patients (52.7 ± 8.9 g/m^2) than in the controls (48.7 ± 8.4 g/m^2, p = 0.032, Table 2). MVR was increased in the T2DM patients (T2DM, 0.88 ± 0.19 g/mL; controls, 0.77 ± 0.16 g/mL, p = 0.007). There were no significant differences between the groups for EDVi, ESVi, or SVi (Table 2). T2DM patients demonstrated a greater ECV than the controls (T2DM, 28.7 ± 3.3%; controls, 26.7 ± 2.7%, p = 0.005) and a similar native T1 and post-contrast T1 (Table 2).

Despite a normal LV ejection fraction (T2DM, 58.5 ± 5.3%; controls, 58.4 ± 5.2%, p = 0.919), the peak diastolic longitudinal strain rate (PDSRL, T2DM, 1.1 ± 0.2/s; controls, 1.2 ± 0.3/s, p = 0.031, Table 3) was impaired in the T2DM patients. There were no significant differences in the other LV mechanics parameters (Table 3).

Relationship between LV mechanics and fractal dimension of LV trabeculations

A reduced PDSRL was associated with an increased LVMMi (sβ = − 0.226, p = 0.033), MVR (sβ = − 0.258, p = 0.015), mean apical FD (sβ = − 0.305, p = 0.004, Fig. 3a), and max. apical FD (sβ = − 0.256, p = 0.016, Fig. 3b), but not with LVECV or EDVi (all p > 0.05). In the stepwise multivariate regression model that included the LVMMi, MVR, max. apical FD, and mean apical FD, only the mean apical FD was an independent determinant of the PDSRL (p = 0.004). After adjusting for age, gender and BMI, the mean apical FD remained independently associated with the PDSRL (p = 0.036). Figure 4 shows

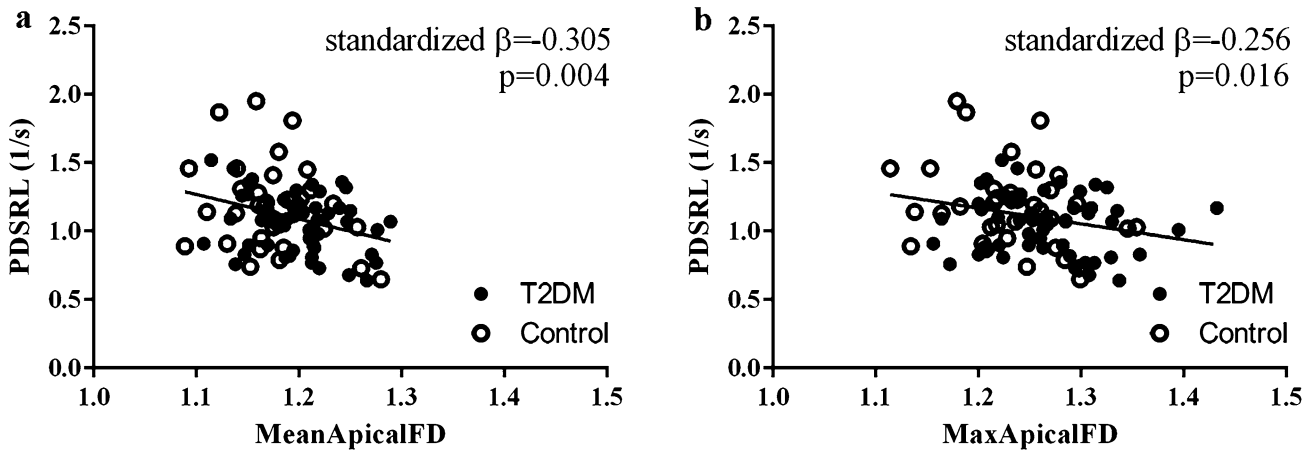

Fig. 3 Relationship between endocardial remodeling and LV subclinical diastolic dysfunction. An elevated mean apical fractal dimension (FD, **a**) and max. apical FD (**b**) are associated with a reduced longitudinal peak diastolic strain rate

representative examples of the FD and PDSRL in a control and a patient with T2DM.

Intra- and inter-observer reproducibility

Summaries of the ICC values and mean differences in intra- and inter-observer reproducibility are shown in Table 4.

Discussion

In this study, we assessed the usefulness of 3T CMR for providing information on LV myocardial structural remodeling and dysfunction in T2DM patients with normotension. We found that the MMi and MVR were increased, the mean apical FD and max. apical FD were elevated, and the longitudinal peak diastolic strain rate was reduced in the T2DM patients compared with the normal controls. Furthermore, the MVR is an independent determinant of the mean apical FD and max. apical FD, suggesting a link between LV concentric hypertrophy and endocardial remodeling. Additionally, the mean apical FD is independently associated with the PDSRL, which indicates that endocardial remodeling may be predictive for subtle LV diastolic dysfunction.

Fractal analysis is a recently introduced technique that employs the FD to objectively assess the extent of PMT to quantify endocardial complexity [19]. In the current study, the max. apical FD in the healthy controls was 1.233 ± 0.055, which is slightly greater than the reference ranges seen in a multi-center healthy population (men, 1.220 ± 0.08; women, 1.194 ± 0.07) [8] and a single-center healthy population (1.199 ± 0.05) [20] and is slightly lower than the recently published reference range in healthy Chinese in Singapore (men, 1.293 ± 0.039; women, 1.261 ± 0.045) [9]. The mean apical FD (1.176 ± 0.043) in our present study is also smaller than that of the healthy Chinese in Singapore (men, 1.235 ± 0.040; women, 1.197 ± 0.044) [9], which indicates that the reference ranges for the mean and max. apical FD remain to be determined in larger, multicenter populations.

This study confirms that T2DM patients with normotension can present with an increased FD consistent with endocardial remodeling. In a previously published study [8], the max. apical FD was elevated in diabetes but not after adjustment for hypertension, a finding that partially counters our own. Notably, the type of diabetes, T1DM and/or T2DM, was not clearly described in that study.

Our own study showed that the MMi and MVR are elevated in T2DM patients, indicating concentric hypertrophy, which is consistent with previous studies [21, 22]. More importantly, the MVR was an independent determinant of the mean and max. apical FD in the present study, suggesting a link between LV concentric hypertrophy and endocardial remodeling. LV trabeculations are comprised of sheets of cardiomyocytes [23] lined by endocardial cells. Our data demonstrated that LV concentric hypertrophy is also associated with increased endocardial fractal complexity in T2DM patients. A previous study in a healthy population that explored the relationship between the FD and MVR showed that the FD was associated with the MMi and EDVi but not with the MVR [9], a finding that is not consistent with our results. Therefore, in the T2DM condition, whether the FD is associated with the MVR needs to be confirmed in future studies.

Another finding in our study was that the PDSRL was significantly decreased in the T2DM patients, indicating subclinical diastolic dysfunction. The question of whether myocardial systolic and diastolic strain and strain rate decrease in T2DM patients is controversial. In Levelt's study [12], the peak circumferential systolic strain was decreased but the peak circumferential diastolic strain rate was not. In

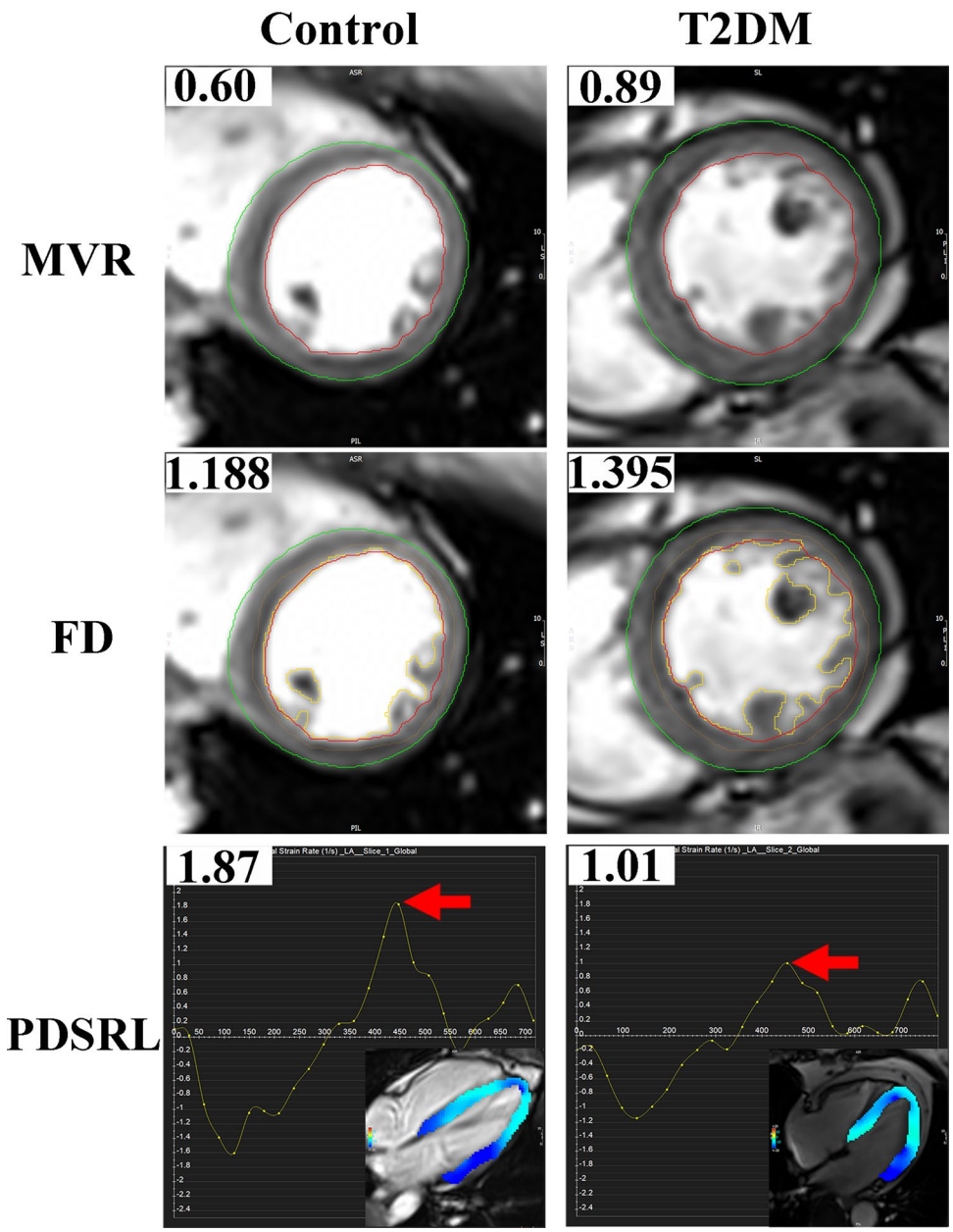

Fig. 4 Representative examples of cardiac cine image, fractal analysis of trabeculations, and myocardial deformation in a control subject, and a patient with T2DM. Top panels: normal control cine image (LV mass-to-end-diastolic volume ratio, MVR = 0.60) versus a patient with T2DM (MVR = 0.89). Middle panels: normal control fractal analysis of trabeculations (max. apical fractal dimension, max. apical FD = 1.188) versus a patient with T2DM (max. apical FD = 1.395). Bottom panels: normal control myocardial deformation (peak longitudinal diastolic strain rate, PDSRL = 1.87) versus a patient with T2DM (PDSRL = 1.01)

another study on participants of the multi-ethnic study of atherosclerosis (MESA) [24], T2DM was associated with reduced circumferential strain. Results on the longitudinal strain and strain rate were not reported in the aforementioned studies. MR-derived tissue tracking technology was used to obtain myocardial strain in our study, whereas MR tagging was employed in the published studies, which may explain these differences. In Cao's study [13], MR-derived tissue tracking technology was used. Diastolic and systolic strain are not impaired in T2DM patients, but they did not report on these factors.

Our results show that the mean apical FD is independently associated with the PDSRL, and the LVECV is not associated with the FD or PDSRL, which indicates that endocardial remodeling may contribute to subtle LV diastolic dysfunction. Based on insights from myocardial fiber orientation, the longitudinal strain and strain rate are governed by the subendocardial fibers, which run parallel to the long axis [25]. Endocardial remodeling, characterized by an increased apical FD, likely involves remodeling of the subendocardial fibers, which explains the relationship between endocardial remodeling and subclinical diastolic dysfunction. Previous studies [9, 24] have also reported a similar mechanical link between LV trabeculations and myocardial deformation in healthy populations. However, in Cai's study [9], the PDSRC and PDSRR, but not the PDSRL, remained independently associated with the mean/max. apical FD. In the other published study of T2DM [24], only the PSC was

Table 4 Intra- and inter-observer reproducibility for LV mechanics and fractal dimension of LV trabeculations

	Intra-observer		Inter-observer	
	Mean difference (95% CI)	ICC (95% CI)	Mean difference (95% CI)	ICC (95% CI)
PSR (%)	0.74 (−5.51, 7.00)	0.866 (0.692, 0.945)	0.73 (−6.29, 7.74)	0.830 (0.620, 0.929)
PSC (%)	−0.10 (−1.53, 1.33)	0.934 (0.842, 0.973)	−0.32 (−1.96, 1.32)	0.907 (0.781, 0.962)
PSSRR (1/s)	−0.02 (−0.88, 0.84)	0.771 (0.507, 0.902)	−0.03 (−0.94, 0.88)	0.754 (0.477, 0.895)
PSSRC (1/s)	0.06 (−0.38, 0.51)	0.566 (0.176, 0.802)	0.07 (−0.40, 0.53)	0.547 (0.150, 0.792)
PDSRC (1/s)	−0.16 (−1.08, 0.76)	0.882 (0.727, 0.952)	−0.16 (−1.12, 0.80)	0.870 (0.701, 0.946)
PDSRC (1/s)	0.04 (−0.39, 0.46)	0.844 (0.648, 0.935)	0.03 (−0.37, 0.43)	0.856 (0.672, 0.940)
PSL (%)	−0.10 (−2.36, 2.17)	0.945 (0.866, 0.978)	−0.25 (−2.70, 2.20)	0.933 (0.838, 0.973)
PSSRL (1/s)	−0.06 (−0.36, 0.25)	0.609 (0.239, 0.824)	−0.06 (−0.35, 0.23)	0.631 (0.272, 0.836)
PDSRL (1/s)	0.04 (−0.25, 0.32)	0.838 (0.637, 0.933)	0.04 (−0.27, 0.35)	0.813 (0.587, 0.922)
LVECV (%)	−0.1 (−0.6, 0.4)	0.950 (0.877, 0.980)	0.3 (−1.1, 1.7)	0.979 (0.947, 0.991)
Max. apical FD	0.002 (−0.006, 0.009)	0.897 (0.758, 0.958)	0.002 (−0.006, 0.009)	0.894 (0.752, 0.957)
Mean apical FD	−0.001 (−0.006, 0.003)	0.959 (0.900, 0.984)	−0.002 (−0.006, 0.003)	0.959 (0.899, 0.983)

PSR peak strain radial, *PSC* peak strain circumf., *PSSRR* peak systolic strain rate radial, *PSSRC* peak systolic strain rate circumf., *PDSRR* peak diastolic strain rate radial, *PDSRC* peak diastolic strain rate circumf., *PSL* peak strain long., *PSSRL* peak systolic strain rate long., *PDSRL* peak diastolic strain rate long., *circumf*. circumferential, *long*. longitudinal, *FD* fractal dimension

studied and it was found to be associated with the max. apical FD. Both these published studies and the present one indicate that endocardial remodeling is a crucial determinant of myocardial mechanical deformation.

Our study had several limitations. First, the overall number of subjects was relatively small. Second, we did not recruit patients with a GFR $\leq$ 30 mL/min/1.7 m^2, and the patients in the study received different treatments. Third, because this is an initial cross-sectional study, we clearly cannot verify whether the observed relationships among concentric hypertrophy, endocardial remodeling, and subtle diastolic dysfunction are causal. Fourth, it may introduce a small risk of misclassification that a single blood pressure measurement and medical history alone were used for exclusion. Finally, although overt coronary artery disease can be easily excluded, subtle coronary artery disease and microvascular dysfunction cannot be identified due to the absence of vasodilator stress first-pass perfusion.

Conclusions

T2DM patients with normotension exhibit LV concentric hypertrophy, endocardial remodeling, and subtle diastolic dysfunction. LV concentric hypertrophy is an independent determinant of endocardial remodeling, a process that may contribute to LV subtle diastolic dysfunction.

Acknowledgements This work was funded by the National Natural Science Foundation of China (Grant Numbers 81471647 and 81571748) and the National Key Research and Development Plan of China (Grant Number 2016YFC0107100) and SWH2016JSTSYB-18.

Compliance with ethical standards

Conflict of interest The authors declare that they have no competing interests.

Ethical approval The Institutional Review Board (IRB) of our hospital approved this study, the reference number was 2016-Scientific-Research-No. 50, and all subjects gave informed consent. This study has therefore been performed in accordance with the ethical standards laid down in the 1964 Declaration of Helsinki and its later amendments.

References

1. Kannel WB, McGee DL (1979) Diabetes and cardiovascular disease. The Framingham study. JAMA 241(19):2035–2038
2. Seferovic PM, Paulus WJ (2015) Clinical diabetic cardiomyopathy: a two-faced disease with restrictive and dilated phenotypes. Eur Heart J 36(27):1718–1727
3. Seferovic PM, Petrie MC, Filippatos GS, Anker SD, Rosano G, Bauersachs J, Paulus WJ, Komajda M, Cosentino F, de Boer RA, Farmakis D, Doehner W, Lambrinou E, Lopatin Y, Piepoli MF, Theodorakis MJ, Wiggers H, Lekakis J, Mebazaa A, Mamas MA, Tschope C, Hoes AW, Seferovic JP, Logue J, McDonagh T, Riley JP, Milinkovic I, Polovina M, van Veldhuisen DJ, Lainscak M, Maggioni AP, Ruschitzka F, McMurray JJV (2018) Type 2 diabetes mellitus and heart failure: a position statement from the Heart Failure Association of the European Society of Cardiology. Eur J Heart Fail. https://doi.org/10.1002/ejhf.1170
4. Gjesdal O, Bluemke DA, Lima JA (2011) Cardiac remodeling at the population level–risk factors, screening, and outcomes. Nat Rev Cardiol 8(12):673–685. https://doi.org/10.1038/nrcardio.2011.154

5. Bluemke DA, Kronmal RA, Lima JA, Liu K, Olson J, Burke GL, Folsom AR (2008) The relationship of left ventricular mass and geometry to incident cardiovascular events: the MESA (multi-ethnic study of atherosclerosis) study. J Am Coll Cardiol 52(25):2148–2155. https://doi.org/10.1016/j.jacc.2008.09.014
6. Dweck MR, Joshi S, Murigu T, Gulati A, Alpendurada F, Jabbour A, Maceira A, Roussin I, Northridge DB, Kilner PJ, Cook SA, Boon NA, Pepper J, Mohiaddin RH, Newby DE, Pennell DJ, Prasad SK (2012) Left ventricular remodeling and hypertrophy in patients with aortic stenosis: insights from cardiovascular magnetic resonance. J Cardiovasc Magn Reson 14:50. https://doi.org/10.1186/1532-429x-14-50
7. Captur G, Karperien AL, Hughes AD, Francis DP, Moon JC (2017) The fractal heart—embracing mathematics in the cardiology clinic. Nat Rev Cardiol 14(1):56–64. https://doi.org/10.1038/nrcardio.2016.161
8. Captur G, Zemrak F, Muthurangu V, Petersen SE, Li C, Bassett P, Kawel-Boehm N, McKenna WJ, Elliott PM, Lima JA, Bluemke DA, Moon JC (2015) Fractal analysis of myocardial trabeculations in 2547 study participants: multi-ethnic study of atherosclerosis. Radiology 277(3):707–715. https://doi.org/10.1148/radiol.2015142948
9. Cai J, Bryant JA, Le TT, Su B, de Marvao A, O'Regan DP, Cook SA, Chin CW (2017) Fractal analysis of left ventricular trabeculations is associated with impaired myocardial deformation in healthy Chinese. J Cardiovasc Magn Reson 19(1):102. https://doi.org/10.1186/s12968-017-0413-z
10. Huckstep OJ, Williamson W, Telles F, Burchert H, Bertagnolli M, Herdman C, Arnold L, Smillie R, Mohamed A, Boardman H, McCormick K, Neubauer S, Leeson P, Lewandowski AJ (2018) Physiological stress elicits impaired left ventricular function in preterm-born adults. J Am Coll Cardiol 71(12):1347–1356. https://doi.org/10.1016/j.jacc.2018.01.046
11. Eitel I, Stiermaier T, Lange T, Rommel KP, Koschalka A, Kowallick JT, Lotz J, Kutty S, Gutberlet M, Hasenfuss G, Thiele H, Schuster A (2018) Cardiac magnetic resonance myocardial feature tracking for optimized prediction of cardiovascular events following myocardial infarction. JACC Cardiovasc Imaging. https://doi.org/10.1016/j.jcmg.2017.11.034
12. Levelt E, Mahmod M, Piechnik SK, Ariga R, Francis JM, Rodgers CT, Clarke WT, Sabharwal N, Schneider JE, Karamitsos TD, Clarke K, Rider OJ, Neubauer S (2016) Relationship between left ventricular structural and metabolic remodeling in type 2 diabetes. Diabetes 65(1):44–52. https://doi.org/10.2337/db15-0627
13. Cao Y, Zeng W, Cui Y, Kong X, Wang M, Yu J, Zhang S, Song J, Yan X, Greiser A, Shi H (2018) Increased myocardial extracellular volume assessed by cardiovascular magnetic resonance T1 mapping and its determinants in type 2 diabetes mellitus patients with normal myocardial systolic strain. Cardiovasc Diabetol 17(1):7. https://doi.org/10.1186/s12933-017-0651-2
14. Alberti KG, Zimmet PZ (1998) Definition, diagnosis and classification of diabetes mellitus and its complications. Part 1: diagnosis and classification of diabetes mellitus provisional report of a WHO consultation. Diab Med 15(7):539–553. https://doi.org/10.1002/(SICI)1096-9136(199807)15:7%3C539::AID-DIA668%3E3.0.CO;2-S
15. Kozor R, Nordin S, Treibel TA, Rosmini S, Castelletti S, Fontana M, Captur G, Baig S, Steeds RP, Hughes D, Manisty C, Grieve SM, Figtree GA, Moon JC (2017) Insight into hypertrophied hearts: a cardiovascular magnetic resonance study of papillary muscle mass and T1 mapping. Eur Heart J Cardiovasc Imaging 18(9):1034–1040. https://doi.org/10.1093/ehjci/jew187
16. Kozor R, Callaghan F, Tchan M, Hamilton-Craig C, Figtree GA, Grieve SM (2015) A disproportionate contribution of papillary muscles and trabeculations to total left ventricular mass makes choice of cardiovascular magnetic resonance analysis technique critical in Fabry disease. J Cardiovasc Magn Reson 17:22. https://doi.org/10.1186/s12968-015-0114-4
17. Wong TC, Piehler KM, Kang IA, Kadakkal A, Kellman P, Schwartzman DS, Mulukutla SR, Simon MA, Shroff SG, Kuller LH, Schelbert EB (2014) Myocardial extracellular volume fraction quantified by cardiovascular magnetic resonance is increased in diabetes and associated with mortality and incident heart failure admission. Eur Heart J 35(10):657–664. https://doi.org/10.1093/eurheartj/eht193
18. Captur G, Radenkovic D, Li C, Liu Y, Aung N, Zemrak F, Tobon-Gomez C, Gao X, Elliott PM, Petersen SE, Bluemke DA, Friedrich MG, Moon JC (2017) Community delivery of semi-automated fractal analysis tool in cardiac mr for trabecular phenotyping. J Magn Reson Imaging 46(4):1082–1088. https://doi.org/10.1002/jmri.25644
19. Captur G, Muthurangu V, Cook C, Flett AS, Wilson R, Barison A, Sado DM, Anderson S, McKenna WJ, Mohun TJ, Elliott PM, Moon JC (2013) Quantification of left ventricular trabeculae using fractal analysis. J Cardiovasc Magn Reson 15:36. https://doi.org/10.1186/1532-429X-15-36
20. Captur G, Lopes LR, Patel V, Li C, Bassett P, Syrris P, Sado DM, Maestrini V, Mohun TJ, McKenna WJ, Muthurangu V, Elliott PM, Moon JC (2014) Abnormal cardiac formation in hypertrophic cardiomyopathy: fractal analysis of trabeculae and preclinical gene expression. Circ Cardiovasc Genet 7(3):241–248. https://doi.org/10.1161/circgenetics.113.000362
21. Velagaleti RS, Gona P, Chuang ML, Salton CJ, Fox CS, Blease SJ, Yeon SB, Manning WJ, O'Donnell CJ (2010) Relations of insulin resistance and glycemic abnormalities to cardiovascular magnetic resonance measures of cardiac structure and function: the Framingham Heart Study. Circulation 3(3):257–263. https://doi.org/10.1161/circimaging.109.911438
22. Heckbert SR, Post W, Pearson GD, Arnett DK, Gomes AS, Jerosch-Herold M, Hundley WG, Lima JA, Bluemke DA (2006) Traditional cardiovascular risk factors in relation to left ventricular mass, volume, and systolic function by cardiac magnetic resonance imaging: the Multiethnic Study of Atherosclerosis. J Am Coll Cardiol 48(11):2285–2292. https://doi.org/10.1016/j.jacc.2006.03.072
23. Sedmera D, Pexieder T, Vuillemin M, Thompson RP, Anderson RH (2000) Developmental patterning of the myocardium. Anat Rec 258(4):319–337
24. Kawel-Boehm N, McClelland RL, Zemrak F, Captur G, Hundley WG, Liu CY, Moon JC, Petersen SE, Ambale-Venkatesh B, Lima JAC, Bluemke DA (2017) Hypertrabeculated left ventricular myocardium in relationship to myocardial function and fibrosis: the multi-ethnic study of atherosclerosis. Radiology 284(3):667–675. https://doi.org/10.1148/radiol.2017161995
25. Hung CL, Verma A, Uno H, Shin SH, Bourgoun M, Hassanein AH, McMurray JJ, Velazquez EJ, Kober L, Pfeffer MA, Solomon SD (2010) Longitudinal and circumferential strain rate, left ventricular remodeling, and prognosis after myocardial infarction. J Am Coll Cardiol 56(22):1812–1822. https://doi.org/10.1016/j.jacc.2010.06.044